

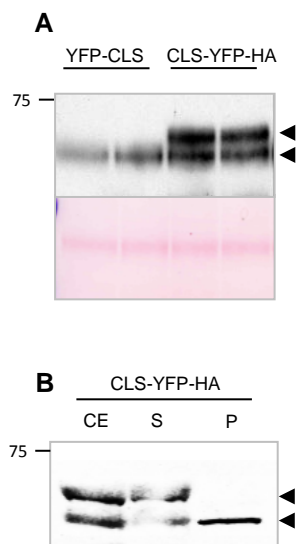


**Supplemental Figure 1.** Sequence comparison of CLS proteins from different species.

(A) A phylogenetic tree of CLS sequences from different species. The tree was created using the online tools in “Phylogeny.fr” (<http://www.phylogeny.fr/version2.cgi/index.cgi>; Dereeper et al., 2008; 2010). Protein sequences were aligned using MUSCLE (3.7) program (Edgar 2004) with the maximum number of iterations of 16, and then adjusted manually. The alignment curation was done with Gblocks 0.91b program (Castresana 2000) (see Supplemental Data Set 1 online). The phylogeny analysis was done using PhyML v3.0 program (Guindon and Gascuel 2003). The statistical test for branch support was done using Approximate Likelihood-Ratio Test (aLRT) with the setting of SH-Like (Anisimova and Gascuel 2006). In aLRT, the model of amino acids substitution was WAG, the number of taxa was 14, the log-likelihood was -1614.71631, the discrete gamma model was yes, the number of categories was 4, the gamma shape parameter was 1.796, and the proportion of invariant was 0.000. Tree Rendering was done using TreeDyn program (Chevenet et al., 2006). Mid-point rooting was used. Scale bar, 1.0 amino acid substitutions per site.

(B and C) Sequence alignment between *Arabidopsis* CLS and CLS homologs from non-plant species (B) and plant species (C). Sequence alignment was performed using the ClustalW2 program. Signal 1 and signal 2 on *Arabidopsis* CLS, which direct the protein to mitochondria and mitochondria/chloroplasts, respectively, are highlighted. The conserved enzymatic activity domain (CDP-alcohol phosphatidyltransferase) is underlined by blue dashed lines.

Accession numbers for the CLS proteins: *Arabidopsis thaliana* (AT4G04870), *Ricinus communis* (XP\_002518507.1), *Populus trichocarpa* (XP\_002305589.1), *Vitis vinifera* (XP\_002264460.1), *Prunus persica* (EMJ12853.1), *Cucumis sativus* (XP\_004134756.1), *Homo sapiens* (NP\_061968.1), *Mus musculus* (NP\_001019556.1), *Danio rerio* (NP\_998096.1), *Xenopus laevis* (NP\_001090462.1), *Drosophila melanogaster* (NP\_001262969.1), *Phaeodactylum tricorutum* (AEZ63317.1), *Saccharomyces cerevisiae* (NP\_010139.1). *Nostoc* sp. PCC 7120 (NP\_488263.1).

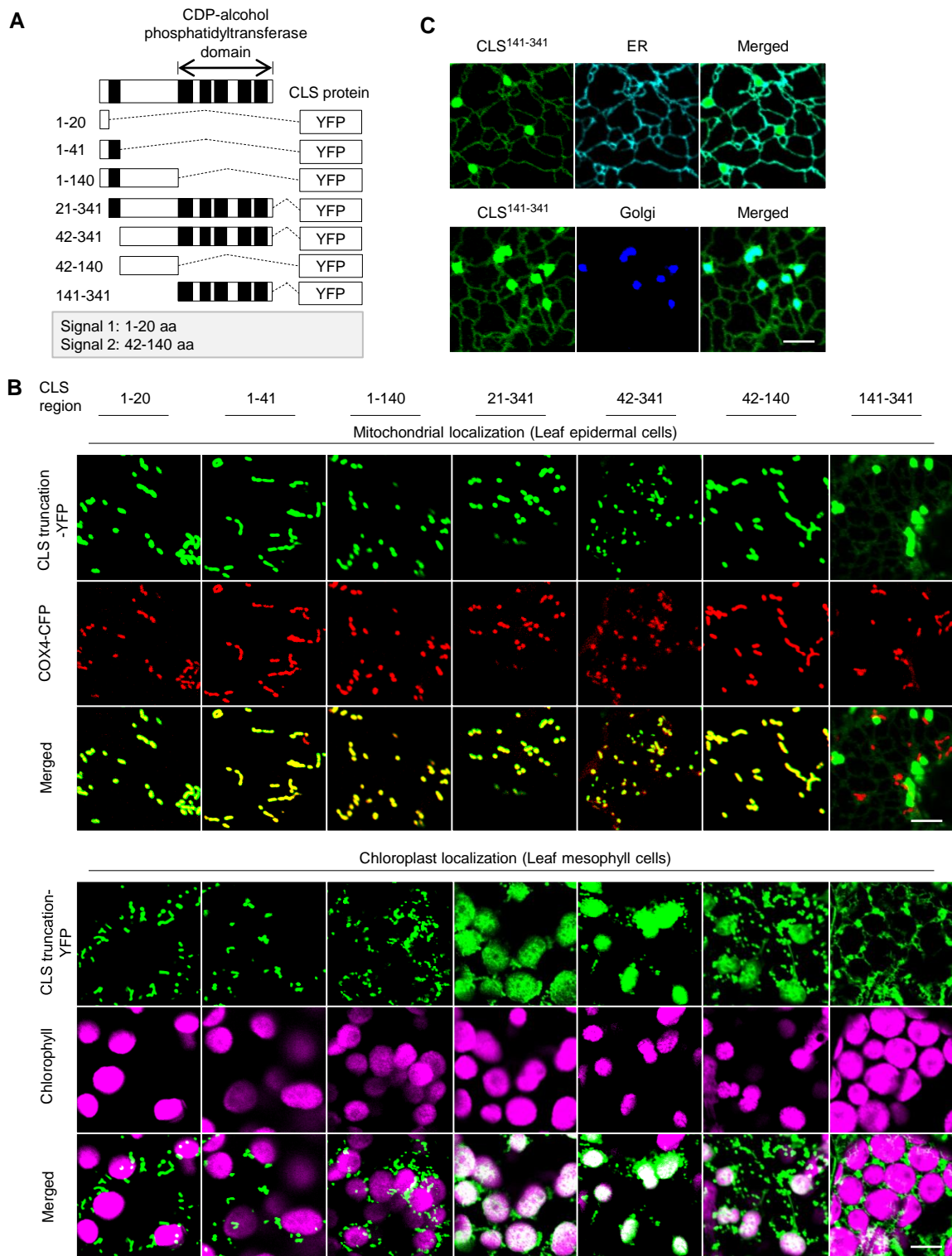


**Supplementary Figure 2.** CLS-YFP-HA is processed upon mitochondrial targeting.

**(A)** Immunoblot analysis of transiently expressed YFP-CLS and CLS-YFP-HA proteins in tobacco leaves, using  $\alpha$ -GFP antibodies. Arrow heads point to the putative precursor and mature form of CLS-YFP-HA. Loading control, large subunit of Rubisco stained by Ponceau S.

**(B)** Immunoblot analysis of CLS-YFP-HA in different subcellular crude fractions. Tobacco leaves transiently expressing CLS-YFP-HA were homogenized on ice in grinding buffer (450 mM Sucrose, 1.5 mM EGTA, 0.2% BSA, 0.6% PVP-40, 10 mM DTT, 0.2 mM PMSF, and 15 mM MOPS/KOH, pH7.4). The homogenized solution is considered crude extract (CE). Chloroplasts and other organelles and particles were sedimented by centrifugation for 10 min at 3,500 g (5 min each time) and 5 min at 6,000 g. Finally, the solution was centrifuged for 10 min at 17,000 g to get a supernatant fraction (S) and a pellet fraction (P) enriched in mitochondria. Arrow heads point to the putative precursor and mature form of CLS-YFP-HA.

Protein markers in kDa are indicated.

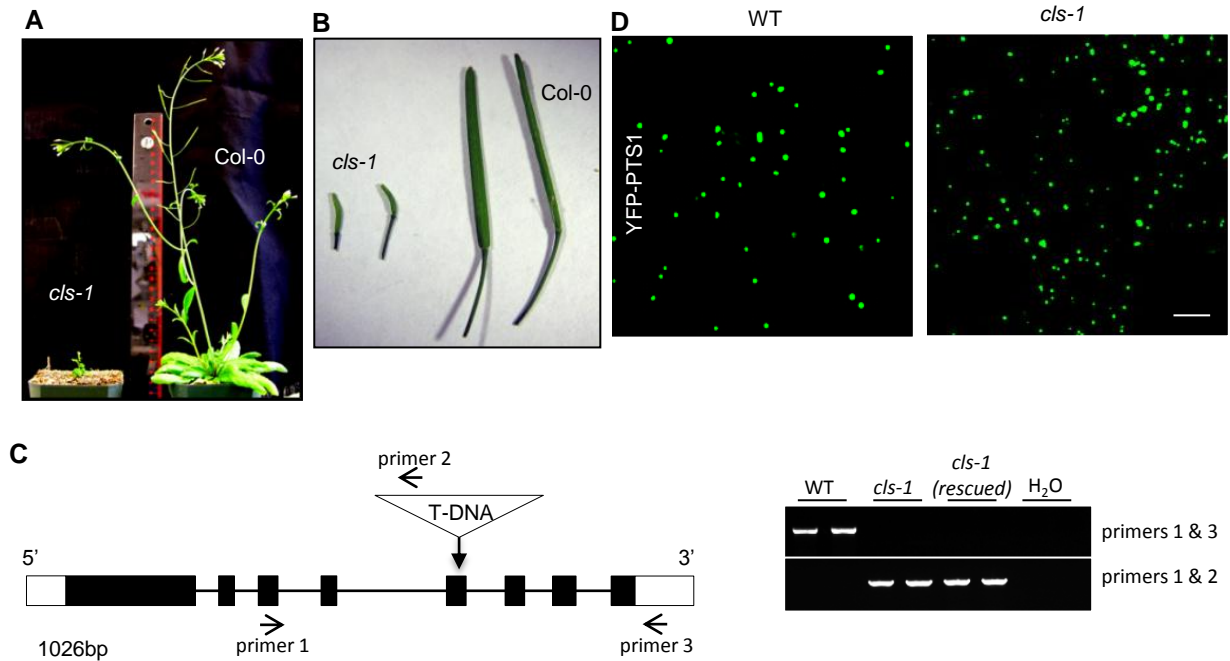


**Supplementary Figure 3.** Analysis of organelle targeting signals on CLS.

(A) Schematics of the CLS protein and deletion constructs. Black box, transmembrane helices predicted by TMHMM server (<http://www.cbs.dtu.dk/services/TMHMM/>).

(B) Confocal images of the localization of fusion proteins between various CLS fragments and YFP transiently expressed in tobacco leaves together with the mitochondrial marker COX4-CFP. Co-localization between COX4-CFP and CLS-YFP fusion proteins were examined in epidermal cells. Co-localization between chloroplast autofluorescent signals and CLS-YFP fusion proteins were examined in mesophyll cells. Scale bars, 5  $\mu$ m.

(C) Localization of CLS<sup>141-341</sup>-YFP to the ER and Golgi. The YFP fusion protein was transiently expressed in tobacco leaves with the ER marker AtWAK2-CFP or Golgi marker GmMan1-CFP (Nelson et al., 2007). Scale bar, 5  $\mu$ m.

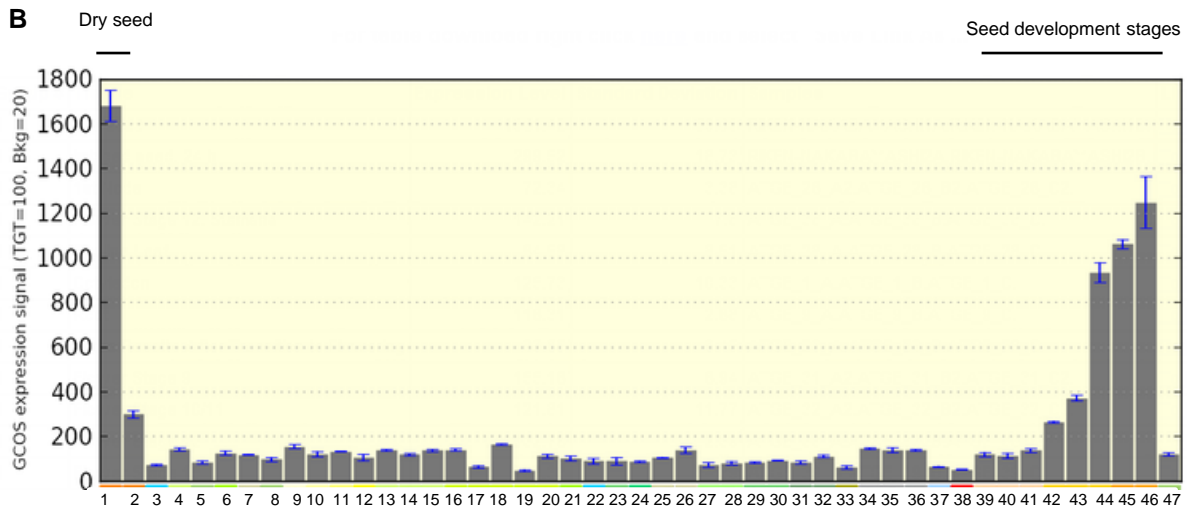
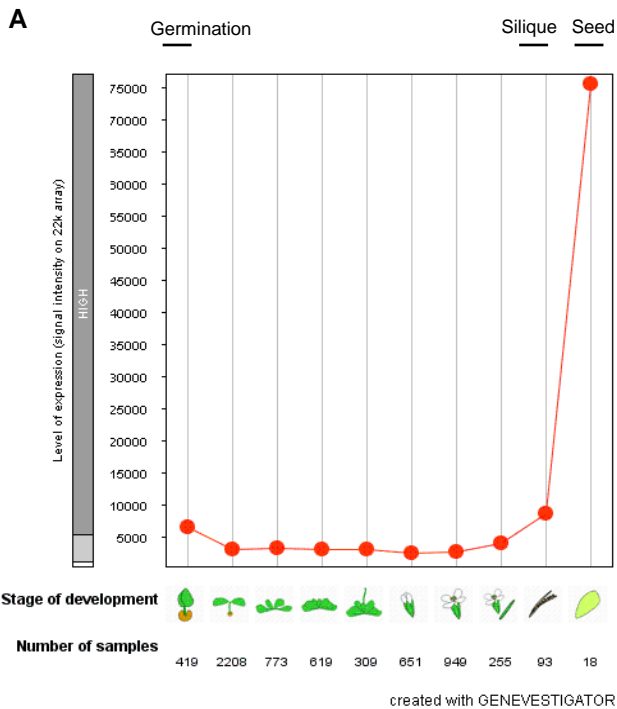


**Supplemental Figure 4.** More characterization of *cls-1*.

**(A-B)** Five-week-old plants (A) and siliques (B).

**(C)** Genotyping of *cls-1* mutant and rescued lines. Schematics of the *Arabidopsis CLS* gene, position of the T-DNA insertions in *cls-1*, and primers used in the genotyping are shown on the left. Genotyping of two independent lines for each genotype is shown on the right.

**(D)** Peroxisomal morphology in five-week-old *cls-1* and wild-type plants expressing the peroxisome marker YFP-PTS1 (SKL). Confocal images were taken from leaf mesophyll cells. Scale bar, 10  $\mu$ m.



**Supplemental Figure 5.** Expression profile of the *Arabidopsis* *CLS* gene.

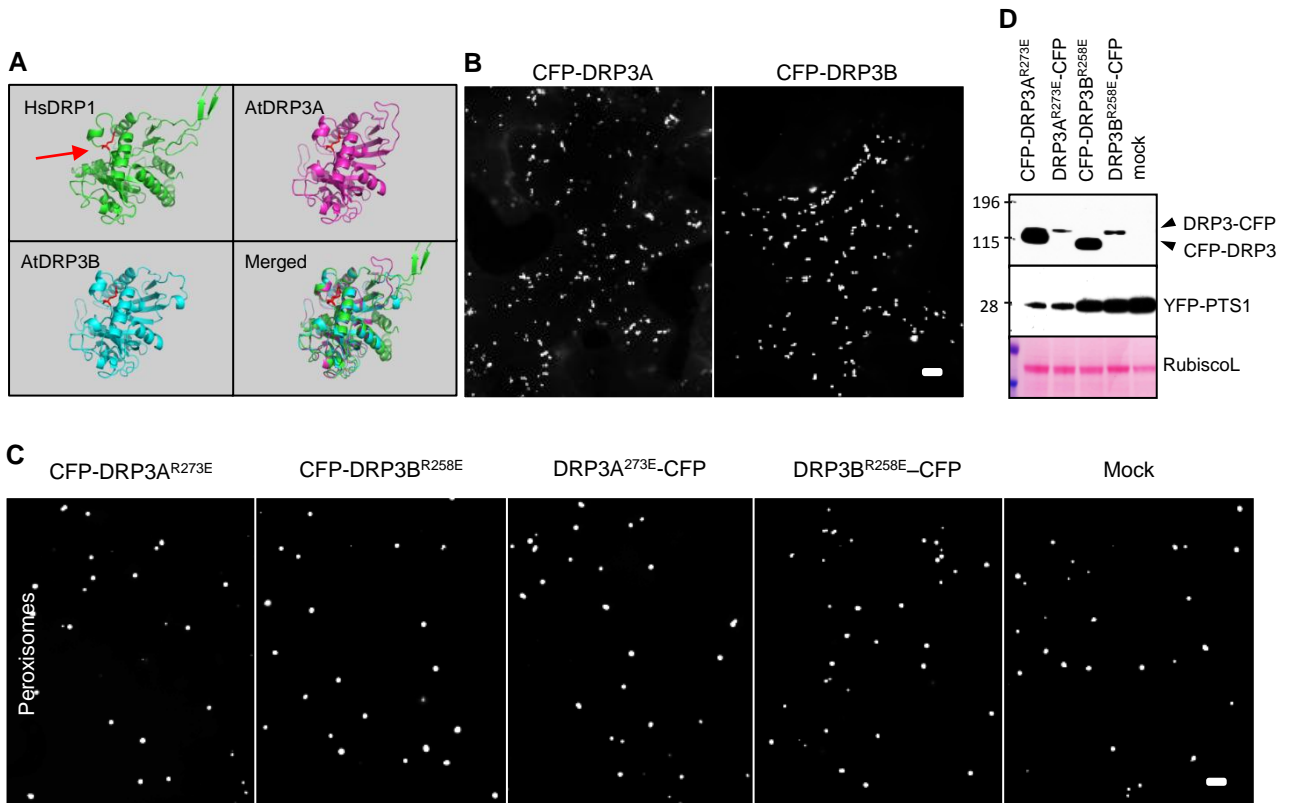
(A) *CLS* expression data from Genevestigator (<https://www.genevestigator.com/>).

(B) *CLS* expression data from *Arabidopsis* eFP browser (bar.utoronto.ca). Developmental stages include: 1, Dry seed; 2, Imbibed seed, 24 h; 3, 1st Node; 4, Flower Stage 12, Stamens; 5, Cauline Leaf; 6, Cotyledon; 7, Root; 8, Entire Rosette After Transition to Flowering; 9, Flower Stage 9; 10, Flower Stage 10/11; 11, Flower Stage 12; 12, Flower Stage 15; 13, Flower Stage 12, Carpels; 14, Flower Stage 12, Petals; 15, Flower Stage 12, Sepals; 16, Flower Stage 15, Carpels; 17, Flower Stage 15, Petals; 18, Flower Stage 15, Sepals; 19, Flower Stage 15, Stamen; 20, Flowers Stage 15, Pedicels; 21, Leaf 1 + 2; 22, Leaf 7, Petiole; 23, Leaf 7, Distal Half; 24, Leaf 7, Proximal Half; 25, Hypocotyl; 26, Root; 27, Rosette Leaf 2; 28, Rosette Leaf 4; 29, Rosette Leaf 6; 30, Rosette Leaf 8; 31, Rosette Leaf 10; 32, Rosette Leaf 12; 33, Senescing Leaf; 34, Shoot Apex, Inflorescence; 35, Shoot Apex, Transition; 36, Shoot Apex, Vegetative; 37, Stem, 2nd Internode; 38, Mature Pollen; 39, Seeds Stage 3 w/ Siliques; 40, Seeds Stage 4 w/ Siliques; 41, Seeds Stage 5 w/ Siliques; 42, Seeds Stage 6 w/o Siliques; 43, Seeds Stage 7 w/o Siliques; 44, Seeds Stage 8 w/o Siliques; 45, Seeds Stage 9 w/o Siliques; 46, Seeds Stage 10 w/o Siliques; 47, Vegetative Rosette.

atDRP3A	MTIEEVSGETPPSTPPSSSTPSPSSSTTNAAPLGSSVIPIVNLQDIFAQLGSQS--TIA	58
atDRP3B	MSVDDLPL-----PSSASAVT---PLGSSVIPIVNLQDIFAQLGSQS--TIA	42
hsDLP1	-----MEALIPVINKLQDVFNVTVGAD---IIQ	24
mmDRP1	-----MEALIPVINKLQDVFNVTVGAD---IIQ	24
dmDRP1	-----MEALIPVINKLQDVFNVTVGSD---SIQ	24
scDNM1	-----MASLEDLIPTVNLQDVMYDSGID---TLD	27
scVPS1	-----MDEHLISTINKLQDALAPLGGGSQSPID	28
atARC5	-----ATARCMAEVSASVTVVEEMAEEDDAAIEERWSLYEAYNELHALAQELETPE	52
atDRP3A	LPQVVVVGSSGKSSVLEALVGRDFLPRGNDICTRRPLVLQLLQTKS-----RAN	109
atDRP3B	LPQVAVVGSSGKSSVLEALVGRDFLPRGNDICTRRPLRLQLVQTKP-----SSD	93
hsDLP1	LPQIVVVGTSQSSGKSSVLESVGRDLLPRGTGIVTRRPLILQLVHVSQ-----EDKRKTT	79
mmDRP1	LPQIVVVGTSQSSGKSSVLESVGRDLLPRGTGIVTRRPLILQLVHVSQ-----EDKRKTT	79
dmDRP1	LPQIVVVGSSGKSSVLESVGRDLLPRGTGIVTRRPLVLQLIYSPL-----DDRENRS	79
scDNM1	LPILAVVGSSGKSSILETLVGRDFLPRGTGIVTRRPLVLQLNINISPNPLIEEDDNSV	87
scVPS1	LPQITVVGSSGKSSVLENIVGRDFLPRGTGIVTRRPLVLQLINRRPKKSEHAKVNQTA	88
atARC5	APAVLVVGQQTGKSSALVEALMGFQFNHVGGGKTRRPIITLHMKYDPQ-----	100
atDRP3A	GGSD-----DEWGEFR-HLPETRFYDFSEIRREIEAET	141
atDRP3B	GGSD-----EEWGEFLHHDVPRRIYDFSEIRREIEAET	126
hsDLP1	GEEN-----GVEAEWGWKFL-HTKNKLYTDFDEIRQEIENET	115
mmDRP1	GEENDPATWKNRSH-----LSKGVAEWGWKFL-HTKNKLYTDFDEIRQEIENET	128
dmDRP1	AENG-----TSNAEWWGRFL-HTK-KCFTDFDEIRKEIENET	114
scDNM1	NPHDEVTKISGFAGTKPLEYR--GKERNHADEWGEFL-HIPGKRFYDFDDIKREIENET	144
scVPS1	NELIDLNINDDDKKKDESGKHQNEGQSEDNKEEWGEFL-HLPGKKFYNFDEIRKEIVKET	147
atARC5	-----CQFPPLCHLGSDD-DPSVSLPKSLSQIQAYIEAEN	133
atDRP3A	NRLVGE-NKGVADTQIRLKISSPNVLNITLVDLPGITKVP--VGDQPSDIEARIRTMILS	198
atDRP3B	NRVSGE-NKGVSDIPIGLKIFSPNVLDISLVDLPGITKVP--VGDQPSDIEARIRTMILT	183
hsDLP1	ERISGN-NKGVSPAPIHLKIFSPNVNLTLLVDLPGMTKVP--VGDQPKDIELQIRELILR	172
mmDRP1	ERISGN-NKGVSPAPIHLKVFSPNVNLTLLVDLPGMTKVP--VGDQPKDIELQIRELILR	185
dmDRP1	ERAAGS-NKGCPEPINLKI FSTHVVNLTLLVDLPGITKVP--VGDQPEDIEAQIKELVLK	171
scDNM1	ARIAGK-DKGISKIPINLKVFSPHVLNLTLLVDLPGITKVP--IGEOPPDIEKQIKNLILD	201
scVPS1	DKVTGA-NSGISSVPINLRIYSPHVLTLTLLVDLPLGLTKVP--VGDQPPDIERQIKDMLLK	204
atARC5	MRLEQEPSPFSAKEIIVKVQYKYCPNLTIIDTPGLIAPAPGLKLRALQVQARAVEALVR	193
atDRP3A	YIKQDTCLILAVTPANTDLANSDALQIASIVDPDGHRTIGVITKLDIMDKGTDARKLLLG	258
atDRP3B	YIKEPSCILAVSPANTDLANSDALQIAGNADPDGHRTIGVITKLDIMDRGTDARNHLLG	243
hsDLP1	FISNPNSIILAVTAANTDMATSEALKISREVPDGRRTLAVITKLDLMDAGTDAMDVLGM	232
mmDRP1	FISNPNSIILAVTAANTDMATSEALKISREVPDGRRTLAVITKLDLMDAGTDAMDVLGM	245
dmDRP1	YIENPNNSIILAVTAANTDMATSEALKLAKDVPDGRRTLAVVTKLDLMDAGTDAIDILCG	231
scDNM1	YIATPNCLILAVSPANVDLVNSESLKLAREVDPQGRRTIGVITKLDLMDSGTNALDILSG	261
scVPS1	YISKPNAILSVNAANTDLANS DGLKLAREVDEPGRRTIGVITKLDLMDQGTVDVIDILAG	264
atARC5	AKMQHKEFIILCLEDDSSWSIATTRRIVMQVPELSRTIVVSTKLDTKIPQFSCSSDVEV	253
atDRP3A	NVVPLRLGYGVVNRRCQEDILLNRTVKEALLAEKFFRSHPVYHGLAD--RLGVPQLAKK	316
atDRP3B	KTIPLRLGYGVVNRCSQEDILMNRSIKDALVAEEKFFRSRPVYSGLTD--RLGVPQLAKK	301
hsDLP1	RVIPVKLGIIGVVNRSQLDINNKKSVTDSIRDEYAFQKK--YPSLAN--RNGTKYLART	288
mmDRP1	RVIPVKLGIIGVVNRSQLDINNKKSVTDSIRDEYAFQKK--YPSLAN--RNGTKYLART	301
dmDRP1	RVIPVKLGIIGVMNRSQKDIMDQKHIDDDQMKDEAAFLQRK--YPTLAT--RNGTPYLAKT	287
scDNM1	KMYPLKLGFGVVNRSQQDIQLNKTVVEESLDKEEDYFRKHPVYRTIST--KCGTRYLAKL	319
scVPS1	RVIPPLRYGIPIVNRGQKDIEHKKTI REALENERKFFENHPSYSSKAH--YCGTPYLAKK	322
atARC5	FLSPPASALDSSLLGDSPPFFTSVPSGRVGYGQDSVYKSNDEFKQAVSLREMEDIASLEKK	313

**Supplementary Figure 6.** Alignment of the N terminus (containing the GTPase domain) of mitochondrial/peroxisome division DRP proteins from various species.

The conserved CL-interacting Arg and the three other conserved residues, Lys, Ser and Thr, in the GTPase domain are highlighted. Sequence alignment was performed using the ClustalW2 program. Accession numbers for proteins sequenced used for the alignment: DRP3A (At4g33650), DRP3B (At2g14120), DRP5B/ARC5 (At3g19720), hsDLP1 (O00429.2), mmDRP1 (Q8K1M6.2), dmDRP1 (Q9VQE0.1), scDNM1 (P54861.1), scVPS1 (P21576.2).



**Supplementary Figure 7. Functional association of CL and DRP3 in mitochondrial fission.**

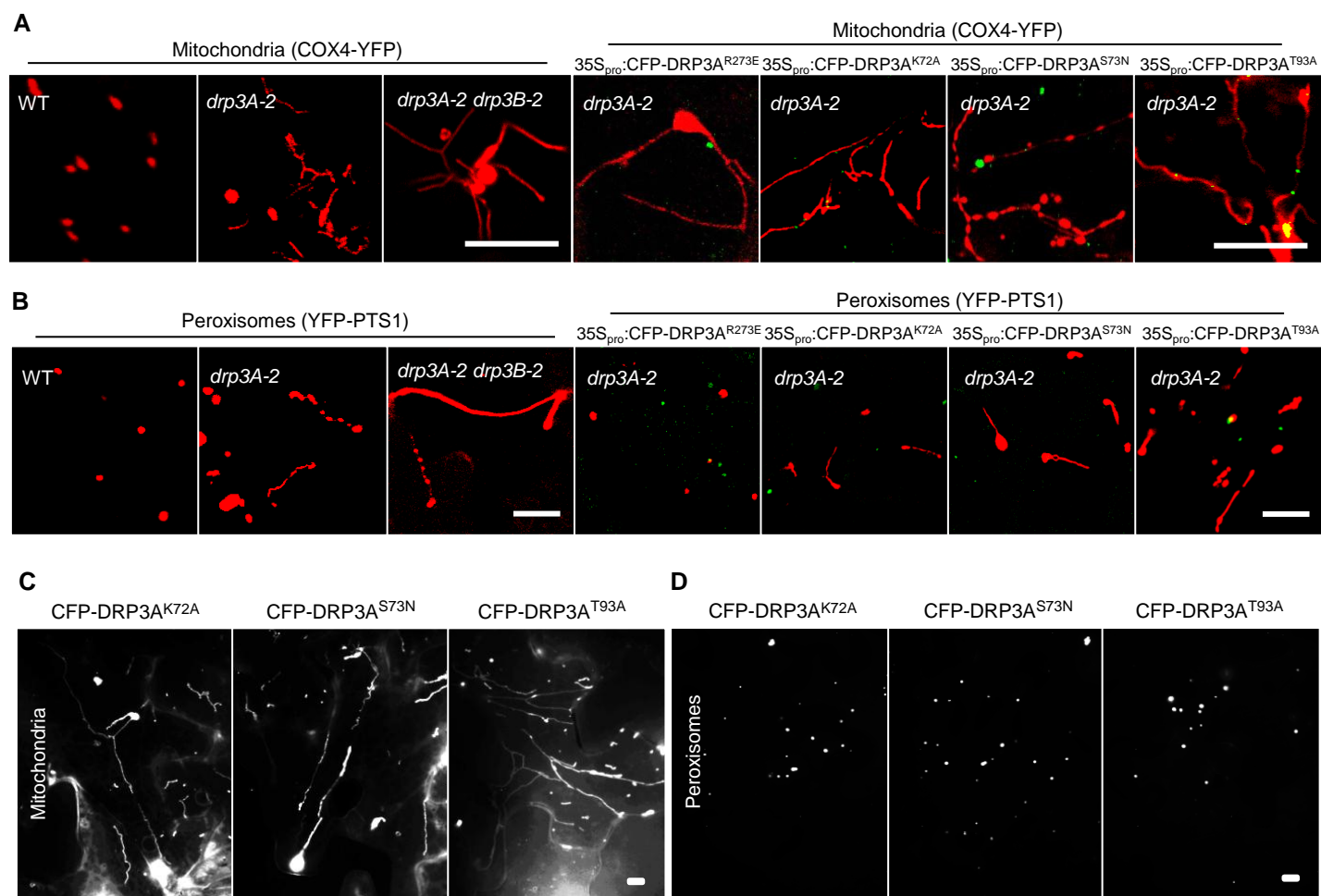
(A) Structural modeling of the GTPase domain from *Arabidopsis* DRP3A (60 to 321 aa) and DRP3B (44 to 306 aa) and human DRP1 (2 to 314 aa). The protein model was generated by SWISS-MODEL (<http://swissmodel.expasy.org>), based on the structure of Dynamin 3 GTPase domain, and visualized with the PyMOL software. The cardiolipin-interacting Arg (R247) is shown in red and indicated by an arrow.

(B) Epifluorescent images showing mitochondrial morphology in tobacco leaf epidermal cells transiently overexpressing wild-type CFP-DRP3A or CFP-DRP3B, together with the mitochondrial marker COX4-YFP. Scale bar, 10  $\mu$ m.

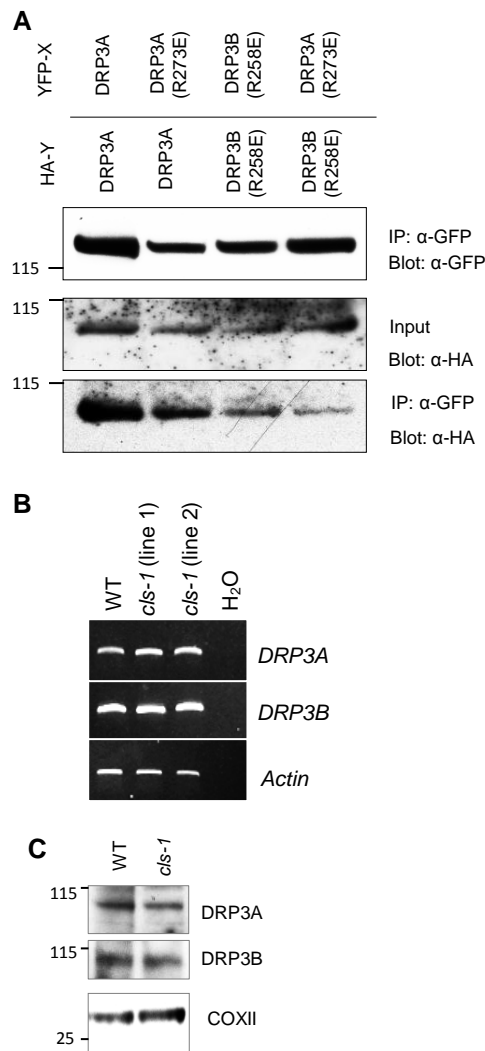
(C) Epifluorescent images showing peroxisome morphology in tobacco leaf epidermal cells transiently overexpressing DRP3A<sup>R273E</sup>-CFP, DRP3B<sup>R258E</sup>-CFP, CFP-DRP3A<sup>R273E</sup>, or CFP-DRP3B<sup>R258E</sup>, together with the peroxisomal marker YFP-PTS1. Scale bar, 10  $\mu$ m.

(D) Immunoblot analysis of DRP3 fusion proteins in crude protein extracts from tobacco leaves co-expressing each CFP-DRP3 (or DRP3-CFP) fusion protein and the peroxisomal marker YFP-PTS1. The proteins were detected by the GFP antibody. Protein size markers in kDa are indicated.





**Supplemental Figure 8.** Analysis of the role of a few conserved residues in mitochondrial and peroxisomal fission. **(A-B)** Mitochondrial (A) and peroxisomal (B) morphologies in leaves of *Arabidopsis* plants in various genetic backgrounds (left) or in *drp3A-2* transiently expressing mutant CFP-DRP3A proteins (right). **(C-D)** Tobacco leaf epidermis overexpressing CFP-DRP3A<sup>K72A</sup>, CFP-DRP3A<sup>S73N</sup> or CFP-DRP3A<sup>T93A</sup> and the mitochondrial (C) or peroxisomal (D) marker.

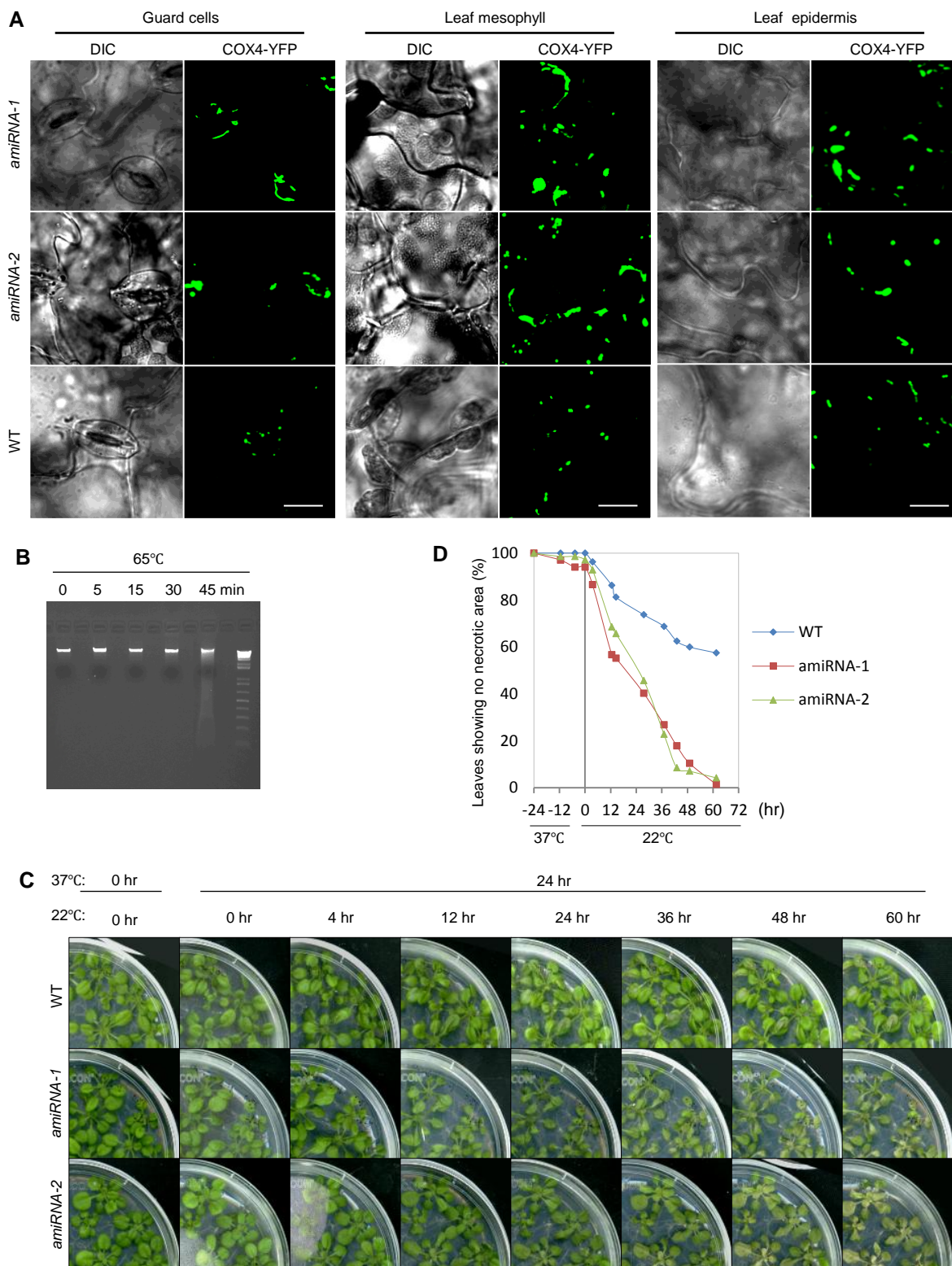


**Supplemental Figure 9.** Analyses of DRP3<sup>R→E</sup> protein self-interaction in tobacco and DRP3 transcript and protein levels in *cls-1*.

(A) Co-IP analysis of YFP- and HA-tagged DRP3 proteins co-expressed in tobacco leaves. IP, immunoprecipitation. Blot, immunoblot.

(B) RT-PCR analysis of *DRP3A* and *DRP3B* transcripts in wild-type and *cls-1* plants. *Actin* mRNA level was included as a loading control.

(C) SDS-PAGE followed by immunoblot analysis of endogenous DRP3 and COXII in *cls-1*, detected by their respective antibodies.



**Supplemental Figure 10.** Mitochondrial phenotypes of *CLS* amiRNA lines and characterization of CL's role in plant response to PCD-inducing stresses.

**(A)** Confocal images showing mitochondrial morphology in the two amiRNA lines used in this study. Scale bars, 10  $\mu$ m.

**(B)** Electrophoresis of genomic DNA from wild-type plants incubated at 65°C for various lengths of time.

**(C)** Three-week-old *Arabidopsis* seedlings subjected to 37°C heat treatment for 24 hours and then left at 22°C.

**(D)** Quantitative analysis of the susceptibility of wild type and *cls* mutants to 24-hr heat stress at 37°C. Percentage of leaves showing no signs of chlorosis or withering was calculated.

**Supplemental Table 1. Primer used in this study.**

Primer	Sequence	Purpose
CLS-Fw-AttB1	GGGGACAAGTTTGTACAAAAAAGCAGG CTTCATGGCGATTTACAGATCTCTAAG	For cloning full length CLS; for RT-PCR analysis of full length CLS & CLS front 453 bp
CLS-Re-AttB2-N	GGGGACCACTTTGTACAAGAAAGCTGG GTCCTATGATCTCTTAATCATAGATATA GG	For cloning full length CLS with stop codon; for RT-PCR analysis of full length CLS
CLS-Re-front	CGCCATTGATATCATATTCGG	For RT-PCR analysis of CLS front 453 bp
CLS-Re-AttB2-C	GGGGACCACTTTGTACAAGAAAGCTGG GTCTGATCTCTTAATCATAGATATAGG	For cloning full length CLS without stop codon
DRP3A-Fw-attB1	GGGGACAAGTTTGTACAAAAAAGCAGG CTTCATGACTATTGAAGAAGTTTCCG	For cloning full length DRP3A
DRP3A-Fw-attB2-N	GGGGACCACTTTGTACAAGAAAGCTGG GTCTTAGAATCCGTATCCATTTTGGTG	For cloning full length DRP3A with stop codon
DRP3A-Re-attB2-C	GGGGACCACTTTGTACAAGAAAGCTGG GTCCAATCCGTATCCATTTTGGTG	For cloning full length DRP3A without stop codon
DRP3B-Fw-attB1	GGGGACAAGTTTGTACAAAAAAGCAGG CTTCATGTCCGTCGACGATCTCCC	For cloning full length DRP3B
DRP3B-Re-attB2-N	GGGGACCACTTTGTACAAGAAAGCTGG GTCTTACATATGAAGCCGTCCGTTC	For cloning full length DRP3B with stop codon
DRP3B-Re-attB2-C	GGGGACCACTTTGTACAAGAAAGCTGG GTCCATATGAAGCCGTCCGTTC	For cloning full length DRP3B without stop codon
CLS-partial -Re-1	GGGGACCACTTTGTACAAGAAAGCTGG GTCTGGTCTGTTTTCCGGTGATTG	For cloning partial CLS
CLS-partial-Re-2	GGGGACCACTTTGTACAAGAAAGCTGG GTCAACAACGGCGAAAAGCTGCGGTG G	For cloning partial CLS
CLS-partial-Re-3	GGGGACCACTTTGTACAAGAAAGCTGG GTCAAACTCTTGACTAATTTCCACC	For cloning partial CLS
CLS-partial-Fw-4	GGGGACAAGTTTGTACAAAAAAGCAGG CTTCATGAGACCATTCTCACCGCCGC TACAGC	For cloning partial CLS
CLS-partial-Fw-5	GGGGACAAGTTTGTACAAAAAAGCAGG CTTCATGCCGTTGTTCCACATTTCTCA C	For cloning partial CLS
CLS-partial-Fw-6	GGGGACAAGTTTGTACAAAAAAGCAGG CTTCATGAAGAGTTTTGTTAATGTGCCG	For cloning partial CLS
DRP3A-R273E-Fw	GTAATGAGTGCCAGGAGGATATTTTG CTAAACCG	Overlapping primer for cloning DRP3A with R273E mutation
DRP3A-R273E-Re	CTGGCACTCATTACAACCTCCACGTAT CCAAGTC	Overlapping primer for cloning DRP3A with R273E mutation
DRP3B-R258E-Fw	GAGTTGTAATGAGAGTCAAGAGGATA TTTTGATG	Overlapping primer for cloning DRP3B with R258E mutation

DRP3B-R258E-Re	TCCTCTTGACTCTCATTTACAACCTCCCA CGTATCC	Overlapping primer for cloning DRP3B with R258E mutation
CLS I miR-s	GATTACACACCCGATAAGAACCCTCTC TCTTTTGTATTCC	For cloning amiRNA CLS
CLS II miR-a	GAGGGTTCTTATCGGGTGTGTAATCAA AGAGAATCAATGA	For cloning amiRNA CLS
CLS III miR*s	GAGGATTCTTATCGGCTGTGTATTAC AGGTCGTGATATG	For cloning amiRNA CLS
CLS IV miR*a	GAATACACAGCCGATAAGAATCCTCTA CATATATATTCCT	For cloning amiRNA CLS
UBQ10-1	TCAATTCTCTCTACCGTGATCAAGATG	For RT-PCR analysis of UBQ10
UBQ10-2	GGTGTCAGAACTCTCCACCTCAAGAG	For RT-PCR analysis of UBQ10
RT-3A-F	GCTGCAAATGCGAGTGATACAAGGTGG G	For RT-PCR analysis of DRP3A
RT-3A-R	CAACTCATCTAGTGCCTGTAAGCTTG C	For RT-PCR analysis of DRP3A
RT-3B-F	CTGCACCAGCTGGAAGCACAAAGCTGG AG	For RT-PCR analysis of DRP3B
RT-3B-R	CCGATTGAGCTTCTAACGGCAGCTCGT C	For RT-PCR analysis of DRP3B
P67_Act7_FP	TTCAATGTCCCTGCCATGTA	For RT-PCR analysis of ACT7 (actin 7)
P68_Act7_RP	TGAACAATCGATGGACCTGA	For RT-PCR analysis of ACT7 (actin 7)
PR-1-LB1	ATGAATTTTACTGGCTATTC	For RT-PCR analysis of PR-1
PR-1-RB1	AACCCACATGTTACGGCGGA	For RT-PCR analysis of PR-1
PR-2-LB1	GCTTCCTTCTTCAACCCACACA	For RT-PCR analysis of PR-2
PR-2-RB1	CTGAACCTTCTTGAGACGGA	For RT-PCR analysis of PR-2
eIF1 $\alpha$ -LB1	GCACAGTCATTGATGCCCA	For RT-PCR analysis of eIF1
eIF1 $\alpha$ -RB1	CCTCAAGAAGAGTTGGTCCCT	For RT-PCR analysis of eIF1
CLS-genotyping-1	CGTACCTTGATCCTCTTGACAG	For genotyping of <i>cls-1</i> and rescued line
CLS-genotyping-2	ATTTTGCCGATTTCCGGAAC	For genotyping of <i>cls-1</i> and rescued line
CLS-genotyping-3	TTAGCGAGGGAACATGTTTTG	For genotyping of <i>cls-1</i> and rescued line
DRP3A-K72A-fw	CAGTGGCGCGTCTAGCGTCTTGAAGC ACTCGTCG	Overlapping primer for cloning DRP3A with K72A mutation
DRP3A-K72A-re	CGCTAGACGCGCCACTGCTTTGGCTTC CAACAAC	Overlapping primer for cloning DRP3A with K72A mutation
DRP3A-S73N-fw	GGCAAGAATAGCGTCCTTGAAGCACTC GTCGGCCG	Overlapping primer for cloning DRP3A with S73N mutation
DRP3A-S73N-re	GACGCTATTCTTGCCACTGCTTTGGCT TCCAACAAC	Overlapping primer for cloning DRP3A with S73N mutation
DRP3A-T93A-fw	ATCTGCGCGCGTGCCTCTTGTCTC CAGCTCC	Overlapping primer for cloning DRP3A with T93A mutation
DRP3A-T93A-re	ACGACGCGCGCAGATATCATTACCAG AGGGAG	Overlapping primer for cloning DRP3A with T93A mutation

<b>Supplemental Table 2. Vector used in this study</b>			
<b>Vector and reference</b>	<b>Description</b>	<b>Construct</b>	<b>Selection of transgenic plants</b>
pDonor 207 (Invitrogen)	Donor vector	all donor plasmids	
pEarleyGate 100 (Earley et al., 2006)	For amiRNA CLS construction	amiRNA CLS	BASTA
pEarleyGate 101 (Earley et al., 2006)	For fusing YFP to N-terminal end of the gene.	YFP-CLS.	BASTA
pEarleyGate 104 (Earley et al., 2006)	For fusing YFP-HA to C-terminal end of the gene.	CLS-YFP-HA	BASTA
pEarleyGate 201 (Earley et al., 2006)	For fusing HA to N-terminal end of the gene.	HA-DRP3A	BASTA
pDest-35S-6xHis-YFP-X (Reumann et al., 2009)	For fusing YFP to N-terminal end of the gene.	YFP-DRP3A, YFP-DRP3B, YFP-DRP3A <sup>R273E</sup> , YFP-DRP3B <sup>R258E</sup>	Kanamycin
pDest-35S-X-YFP-6xHis (Reumann et al., 2009)	For fusing YFP to C-terminal end of the gene.	CLS <sup>1-20</sup> -YFP, CLS <sup>1-41</sup> -YFP, CLS <sup>1-140</sup> -YFP, CLS <sup>21-341</sup> -YFP, CLS <sup>42-341</sup> -YFP, CLS <sup>42-140</sup> -YFP, CLS <sup>141-341</sup> -YFP	Kanamycin
pGWB544 (Nakagawa et al., 2007)	For fusing CFP to C-terminal end of the gene.	CFP-DRP3A, CFP-DRP3B, CFP-DRP3A <sup>R273E</sup> , CFP-DRP3B <sup>R258E</sup> , CFP-DRP3A <sup>K72A</sup> , CFP-DRP3A <sup>S73N</sup> , CFP-DRP3A <sup>T93A</sup>	Hygromycin
pGWB545 (Nakagawa et al., 2007)	For fusing CFP to N-terminal end of the gene.	DRP3A <sup>R273E</sup> -CFP, DRP3B <sup>R258E</sup> -CFP	Hygromycin

### Supplemental References:

- Anisimova, M., and Gascuel, O.** (2006). Approximate likelihood ratio test for branches: A fast, accurate and powerful alternative. *Syst Biol.* **55**, 539-552.
- Castresana, J.** (2000). *Selection of conserved blocks from multiple alignments for their use in phylogenetic analysis.* *Mol Biol Evol.* **17**, 540-552.
- Chevenet, F., Brun, C., Banuls, A.L., Jacq, B., and Chisten, R.** (2006). TreeDyn: towards dynamic graphics and annotations for analyses of trees. *BMC Bioinformatics.* **7**, 439.
- Dereeper, A., Guignon, V., Blanc, G., Audic, S., Buffet, S., Chevenet, F., Dufayard, J.F., Guindon, S., Lefort, V., Lescot, M., Claverie, J.M., and Gascuel, O.** (2008). *Phylogeny.fr: robust phylogenetic analysis for the non-specialist.* *Nucleic Acids Res.* **36** (Web Server issue), W465-469.
- Dereeper, A., Audic, S., Claverie, J.M., Blanc, G.** (2010). *BLAST-EXPLORER helps you building datasets for phylogenetic analysis.* *BMC Evol Biol.* **10**, 8.
- Edgar, R.C.** (2004). MUSCLE: multiple sequence alignment with high accuracy and high throughput. *Nucleic Acids Res.* **32**, 1792-1797.
- Earley, K.W., Haag, J.R., Pontes, O., Opper, K., Juehne, T., Song, K., and Pikaard, C.S.** (2006). Gateway-compatible vectors for plant functional genomics and proteomics. *Plant J* **45**, 616-629.
- Guindon, S., and Gascuel, O.** (2003). A simple, fast, and accurate algorithm to estimate large phylogenies by maximum likelihood. *Syst Biol.* **52**, 696-704.
- Nakagawa, T., Suzuki, T., Murata, S., Nakamura, S., Hino, T., Maeo, K., Tabata, R., Kawai, T., Tanaka, K., Niwa, Y., Watanabe, Y., Nakamura, K., Kimura, T., and Ishiguro, S.** (2007). Improved Gateway binary vectors: high-performance vectors for creation of fusion constructs in transgenic analysis of plants. *Biosci Biotechnol Biochem* **71**, 2095-2100.
- Reumann, S., Quan, S., Aung, K., Yang, P., Manandhar-Shrestha, K., Holbrook, D., Linka, N., Switzenberg, R., Wilkerson, C.G., Weber, A.P., Olsen, L.J., and Hu, J.** (2009). In-depth proteome analysis of Arabidopsis leaf peroxisomes combined with in vivo subcellular targeting verification indicates novel metabolic and regulatory functions of peroxisomes. *Plant Physiol* **150**, 125-143.